IJPSR (2019), Volume 10, Issue 4 (Research Article)

INTERNATIONAL JOURNAL OF PHARMACEUTICAL SCIENCES AND RESEARCH

Received on 05 February 2019; received in revised form, 07 March 2019; accepted, 09 March 2019; published 01 April 2019

NANOEMULSION-BASED CAMPHOR OIL CARRYING IFOSFAMIDE: PREPARATION, CHARACTERIZATION, AND *IN-VITRO* EVALUATION IN CANCER CELLS

Sahar M. AlMotwaa [1, 2], Mayson H. Alkhatib [* 1], Huda M. Alkreathy [3]

Department of Biochemistry, Faculty of Science [1], Department of Pharmacology, Faculty of Medicine [3], King Abdulaziz University, Jeddah, Saudi Arabia.
Department of Chemistry [2], College of Science and Humanities, Shaqra University, Shagra, Saudi Arabia.

Keywords:

Z-average diameter, Zeta potential, Antiproliferation activity, Half-maximal inhibitory concentration, Cytotoxicity, Apoptosis

Correspondence to Author:
Mayson H. Alkhatib

Department of Biochemistry, Faculty of Science, King Abdulaziz University, P.O. Box 42801, Jeddah 21551, Saudi Arabia.

E-mail: mhalkhatib@kau.edu.sa

ABSTRACT: Formulating the essential oils with the chemotherapeutic agents in nanocarrier may develop a potent effect on the cancer cells. A nanoemulsion consisting of the camphor oil (CAM-NE) and Ifosfamide (IFO)-loaded in CAM-NE (CAM-IFO) were physically characterized by the zetasizer and evaluated for *in-vitro* antiproliferative activity against MCF-7 breast and HeLa cervical cancer cell lines. The cell growth inhibition, cell morphological changes, and apoptosis of the cancer cells, subjected into the CAM-NE, CAM-IFO and the free-drug (IFO), were examined by the MTT assay, light microscopy, and DAPI stain, respectively. It has been found that the dispersed nanodroplets of CAM-NE had mean particle diameter and zeta potential of 34.975 ± 9.35 nm and -13.75 ± 1.06 mV, respectively, which had got enlarged to 96.235 ± 9.00 nm and -22.00 ± 0.49 mV, respectively, when IFO was incorporated (CAM-IFO). The results of the cell growth inhibition and cellular uptake have demonstrated that CAM-IFO has the highest cytotoxic effect on both tested cells when compared with CAM-NE and IFO. These findings suggest that the combination therapy of IFO with NE-based CAM oil has potential anticancer activity.

INTRODUCTION: Ifosfamide (IFO), a chemotherapeutic agent used in the treatment of a variety of pediatric tumors, especially sarcomas, is usually combined with some different agents such as vincristine, actinomycin or doxorubicin. Although it is considered to be an analog of cyclophosphamide, IFO appears to have a specific activity in some tumor types, for example, rhabdomyosarcoma [1].

QUICK RESPONSE CODE

DOI: 10.13040/IJPSR.0975-8232.10(4).2018-26

The article can be accessed online on www.ijpsr.com

DOI link: http://dx.doi.org/10.13040/IJPSR.0975-8232.10(4).2018-26

The whitish powdery IFO ($C_7H_{15}Cl_2N_2O_2P$, M. wt = 261 g/mol) hasp Ka less than 2.5 with basic characters and log P 1.68. [2, 3] IFO, belongs to the Biopharmaceutics Classification System (BCS) Class III drug, has a water solubility about 100 mg/ml with a melting point of 40 °C and noticeable hygroscopic properties [4]. IFO drug undergoes hydroxylation at the oxazaphosphorine ring's carbon-4 position to become activated in the liver through the cytochrome P450 (CYP3A4 and CYP2B6) enzymatic system yielding cytotoxic agent called IFO mustards that alkylates DNA at the guanosine's N-7 position [1].

The most serious complications associated with the administration of IFO are mainly neurotoxicity and nephrotoxicity which result from the formation of

IFO metabolite chloroacetaldehyde [1]. Several previous studies have attempted to incorporate IFO into different nanocarriers with the aim to enhance its stability, cellular uptake and permeability to improve its therapeutic efficacy. IFO was formulated in nanostructured lipid nanoparticles, span 80 nanovesicles, self-assembled polymeric nanoparticles, solid-lipid nanoparticle, and self-micro emulsifying drug delivery systems [5, 7, 8, 9]. In the current study, we have proposed a new nanoemulsion (NE) formulation that promotes the combination between the essential oil, camphor (CAM), and IFO with the aim to potentiate the IFO's toxicity on cancer cells and eliminate its adverse side effects.

IFO can't be administrated for human orally due to the neurotoxicity. It is only available for human intravenously which is also associated with nephrotoxicity [1]. CAM oil was involved in formulating microemulsion and NE [10, 11] to deliver many hydrophobic drugs. Few animal studies have demonstrated the CAM potential in the treatment of cancer. However, many studies elaborated the beneficial properties of CAM which included the improvement of immune function, enhancement of enzymatic breakdown of carcinogens and the increased susceptibility of cancer cells to radiation [12].

Moreover, previous studies showed that encapsulation of essential oils into emulsion due to the hydrophobic nature of oil leads to higher solubility and dispersibility in aqueous media besides the reduction of the organoleptic (hydrophobic) properties in the food systems [13]. It has been demonstrated that NE systems increased the retention of the drug in the body by increasing the drug release and reducing clearance and volume of distribution and hence enhanced the bioavailability and reduced the amount of the drug required for the therapeutic action [14, 15, 16, 17]. The objective of the current study was to formulate IFO in NE-based CAM oil and to assess its anticancer activity in the MCF-7 breast cancer cells and HeLa cervical cancer cells.

MATERIALS AND METHODS:

Chemicals and Subjects: The 3 (4, 5 dimethyl thiazole-2-yl) -2, 5-diphenyltetrazolium bromide (MTT) and Coomassie brilliant blue were obtained from Biomatik (Ontario, Canada). All of the required tissue culture chemicals were supplied by Lonza Walkersville (USA). The 4′, 6-diamidino-2-phenylindole (DAPI) dihydrochloride was obtained from Invitrogen Life Technologies (New York, US). IFO was purchased from Baxter, US. Span 20 and tween 80 were obtained from Sigma (Missouri, US). The human cervical cancer cell line (HeLa), human breast adenocarcinoma cell line (MCF-7) were procured from the American Type Tissue Culture Collection (Manassas, VA, USA).

Formation of the NEs Using the Phase Diagram: To prepare the NEs, it is necessary to construct a pseudo-ternary phase diagram at different weight fractions of CAM oil, water, and a surfactant mixture blended at a fixed ratio of 2:1 of tween 80 to span 20, respectively. The tween 80 and span 20 are nonionic surfactants that enhance solubilization when combined with oils [18]. Previously found that surfactant mixture of tween 80 and span 20 provide higher water solubilization [19] and tween 80 makes the nanoparticles most stably dispersed in aqueous solutions with preventing aggregation [20].

The phase diagram reveals the emulsion (EM) regions at which the resulted formula may get converted to NE. The oil-in-water (O/W) NE formulas (CAM-NE) were produced by selecting one of the formed EM formulas, which consisted of 5.5% (w/w) surfactant mixture, 1.8% (w/w) CAM oil and 92.7% (wt/wt) water, followed by vortexing and heating at 70 °C until it becomes clear and transparent. The stock solutions of 19 mM of IFO (5 mg IFO/ml distilled water) and CAM-IFO (5mg IFO/ml CAM-NE) were prepared by directly dissolving IFO in the desired solution. Then, serial dilutions of the stock solution were produced by using culture media to prepare the required concentration.

Determination of the Particle Size and Charge of the NE Droplets: The sizes and charges of the NE droplets, represented by z-average diameters and zeta potentials, respectively, were measured by Zeta Sizer (Malvern Instruments, Malvern, UK). Measurements were implemented at 25 °C.

Cell Culture: MCF-7 and HeLa cells were seeded in a 25 cm^2 cell culture flask, containing Dulbecco's modified Eagle medium (DMEM), 10%

(v/v) fetal bovine serum (FBS) and 1% (v/v) penicillin-streptomycin, and incubated in a 5% CO_2/ 95% humidified atmosphere at 37 °C. The media were changed every 48 h until confluence followed by washing with 2 ml of phosphate buffered saline (PBS, pH7, 10mM), detachment by adding 2 ml of trypsin, and incubation at 37 °C.

MTT Assay for Toxicity Detection of NEs on the Cancer Cells: In each well of a 96-well plate, 100 µl of 10,000 cells seeded in the culture media were incubated overnight at 37 °C in a CO_2 incubator for cell attachment. Then, cells were subjected to 100 µl of the tested formulas and kept in a CO_2 incubator at 37 °C. The toxic amounts of CAM-NE and CAM-IFO formula were in the range between 26 to 261 µg/ml, while the IFO amounts were in the range between 700 to 3100 µg/ml. After 24h of incubation, a 5 µl of MTT reagent was inserted with gentle mixing into each well and left for 3 to 4h at 37 °C in a CO_2 incubator.

After the removal of the supernatant, a 100 µl of dimethyl sulfoxide (DMSO) was added and kept for 2h. The Absorbance (Abs) of the treated cells was read at 570 nm using a microplate reader (BioTek, US). Wells, included culture media, were considered negative control while culture media containing cells served as a positive control. The following equation determined the percentages of cell viabilities:

Cell viability (%) = Abs of treated cells – Abs of negative cell / Abs of positive cell - Abs of negative cell × 100

Light Microscopy for the Visualization of the Cell Death: The phase contrast inverted microscope (Olympus 1X51, Japan) was utilized to detect the signs of apoptosis and necrosis in the treated HeLa and MCF-7 cells. 100 µl of the growth media containing 10,000 cells, subjected into 100 µl of the tested formulas, were seeded into each well of 96-well plate. After 24 h incubation in a CO_2 incubator at 37 °C, cells were washed twice with 100 µl of PBS followed by fixation through the addition of 100 µl of 4% formaldehyde for 5 min. After the removal of the fixation solution, cells were washed with 100 µl of PBS and stained with 100 µl of 10% Coomassie blue for 10 min. Following the removal of the stain, cells were washed with 100 µl of distilled water twice and left to dry at 25 °C.

DAPI Stain for the Detection of Apoptosis: DAPI penetrates the cells and gets attached into the nucleus due to the interactions with A-T rich regions in DNA to give an intense blue fluorescent dye. 5×10^4 cells per 500 µl of growth media were cultured in each well of 24 well-plates and subjected into 500 µl of the tested formula. Following 24 h incubation in a CO_2 incubator at 37°C, cells were inserted with 300µl of PBS, fixed by 200 µl of formaldehyde and stained with 300 µl of 300 nM of DAPI solution. Following incubation for 1-5 min at 25 °C, cells were visualized with the inverted fluorescent microscope (Leica CRT6000, Germany). Image J 1.43 n software (Rasband, W.S., Image J, National Institutes of Health, US) was utilized to measure the percentages of fluorescent intensity.

Statistical Analysis: The differences between the samples were identified statistically by using one-way analysis of variance (ANOVA) (MegaStat, version 10.3, Butler University, Indianapolis, IN). The differences were considered when P-value <0.05.

RESULTS:

Formulation and Physical Characterization of the CAM-NE and CAM-IFO: As shown in **Fig. 1**, the phase diagram was constructed at different weight fractions of water, CAM oil and tween 80/ span 20 to determine the one-phase emulsion region that might be converted into CAM-NE. On the left of the phase diagram, a two-phase region on the bottom was slightly larger than the three-phase region while the one-phase region was located on the top of the phase diagram.

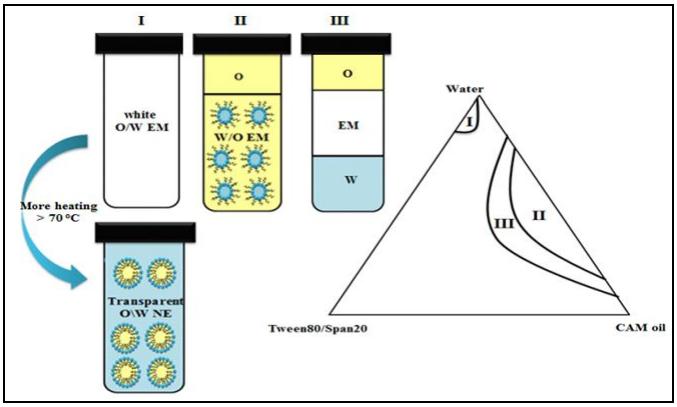

FIG. 1: PSEUDO TERNARY PHASE DIAGRAM CONSTRUCTED BY DIFFERENT WEIGHT FRACTIONS OF WATER, CAMPHOR (CAM) OIL AND A CONSTANT RATIO OF 2:1 OF TWEEN 80 \ SPAN 20. Em: emulsion; O/W: oil-in-water; W/O: water-in-oil and NE: nanoemulsions

TABLE 1: ZETA SIZER MEASUREMENTS OF THE PRODUCED NES FORMULAS

Formula	Zeta Potential (mV)	z-Average Diameter (nm)
CAM NE	-13.75 ± 1.06	34.975 ± 9.35
CAM IFO	-22.00 ± 0.49***	96.235 ± 9.00***

*** The differences between CAM-NE and CAM-IFO in zeta potential and z-average diameter were highly significant (P < 0.001, measured by the independent *t*-test)

In the one-phase (O/W emulsion) region, the formula, consisting of the weight fractions of 4% surfactant, 1.5% co-surfactant, 1.8% LEM or SAL oil and 92.7% water, was transformed into transparent CAM-NE when subjected into further heating (>70 °C) and vortexing for one hour. The CAM-IFO was produced by directly solubilizing 5mg of IFO in 1mLCAM-NE. As exhibited in **Table 1**, the physical properties of the CAM-NE and CAM-IFO were identified by the zeta sizer. Both of the magnitudes of the negatively charged zeta potential and z-average diameter of CAM-NE have markedly enhanced when loaded with IFO (CAM-IFO).

Cell Growth Inhibition: The anti-proliferative effects of CAM-NE, CAM-IFO, and IFO formulas were performed in MCF-7 and HeLa cells using MTT assay at various concentrations for 24 h. As shown in **Fig. 2A** and **3A**, the cell growth inhibition in both cells, subjected to the CAM-IFO, exhibited a significant increase when compared with the CAM-NE and the IFO. In particular, the IC_{50}'s of the CAM-IFO was the least, but it was the maximum for the free IFO in both cells.

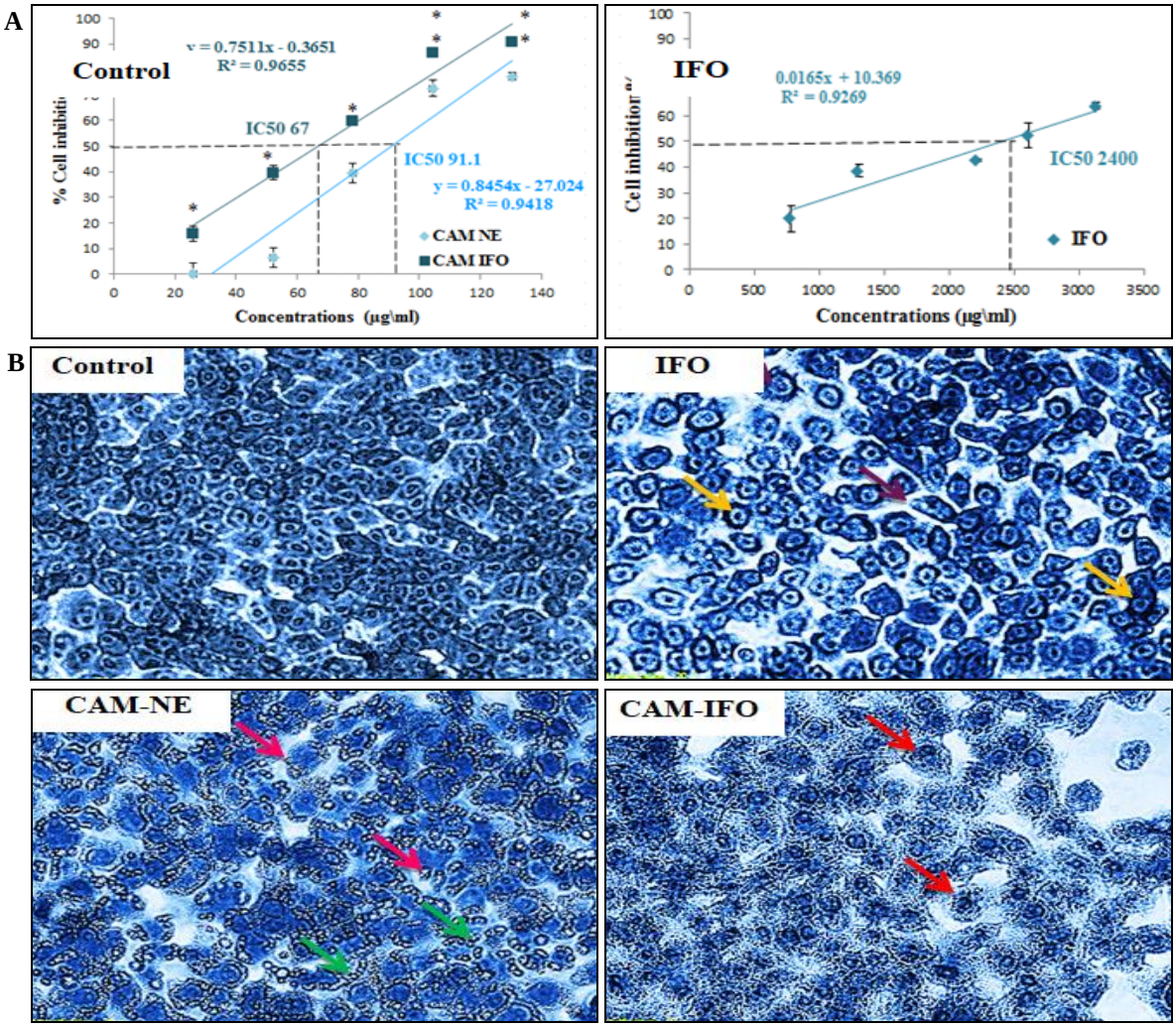

FIG. 2: (A) MTT ASSAY DETERMINATION OF THE PERCENTAGES OF MCF-7 CELLS GROWTH INHIBITION SUBJECTED INTO THE TESTED FORMULAS FOR 24 h AT DIFFERENT CONCENTRATIONS OF CAM-NE, CAM-IFO, AND IFO. (B) LIGHT MICROSCOPY IMAGES OF THE UNTREATED MCF-7 CELLS (CONTROL) AND THE TREATED MCF-7 CELLS WITH THE IC_{50}'s OF 2400, 91.1 AND 67.0 µg/ml FOR IFO, CAM-NE, AND CAM-IFO, RESPECTIVELY. Error bars display the standard deviation; P-values were measured by the independent *t*-test; * p<0.05; ** 0.001<P<0.05. Images were magnified at 400X. Purple, orange, pink, green and red arrows represent membrane blebbing, chromatin condensation, cellular membrane integrity, vesicles, and ghost cell, respectively.

Cell Morphology of MCF-7 and HeLa Cells: To examine the morphological changes of the HeLa and MCF-7 cells subjected to the IC_{50}'s of the free IFO, CAM-NE, and CAM-IFO, the light microscopy images were utilized as exhibited in **Fig. 2B** and **3B**. The MCF-7 cells have endured cell membrane shrinkages with chromatin condensation when treated with free IFO **Fig. 2B**. In contrast, there were obvious changes in the cells treated with the two NE formulas. CAM-NE treated cells revealed apparent late signs of apoptosis such as loss of cellular membrane integrity and stimulation of vesicle formation while some of the CAM- IFO treated cells were completely killed and appeared as ghost cells. According to the light microscopy images of the HeLa cells **Fig. 3B**, irregular cell shape and membrane blebbing were seen when free IFO was applied into the cells. On the other hand, cells treated with CAM-NE and CAM-IFO has exhibited the formation of vesicles and enlargement in their size.

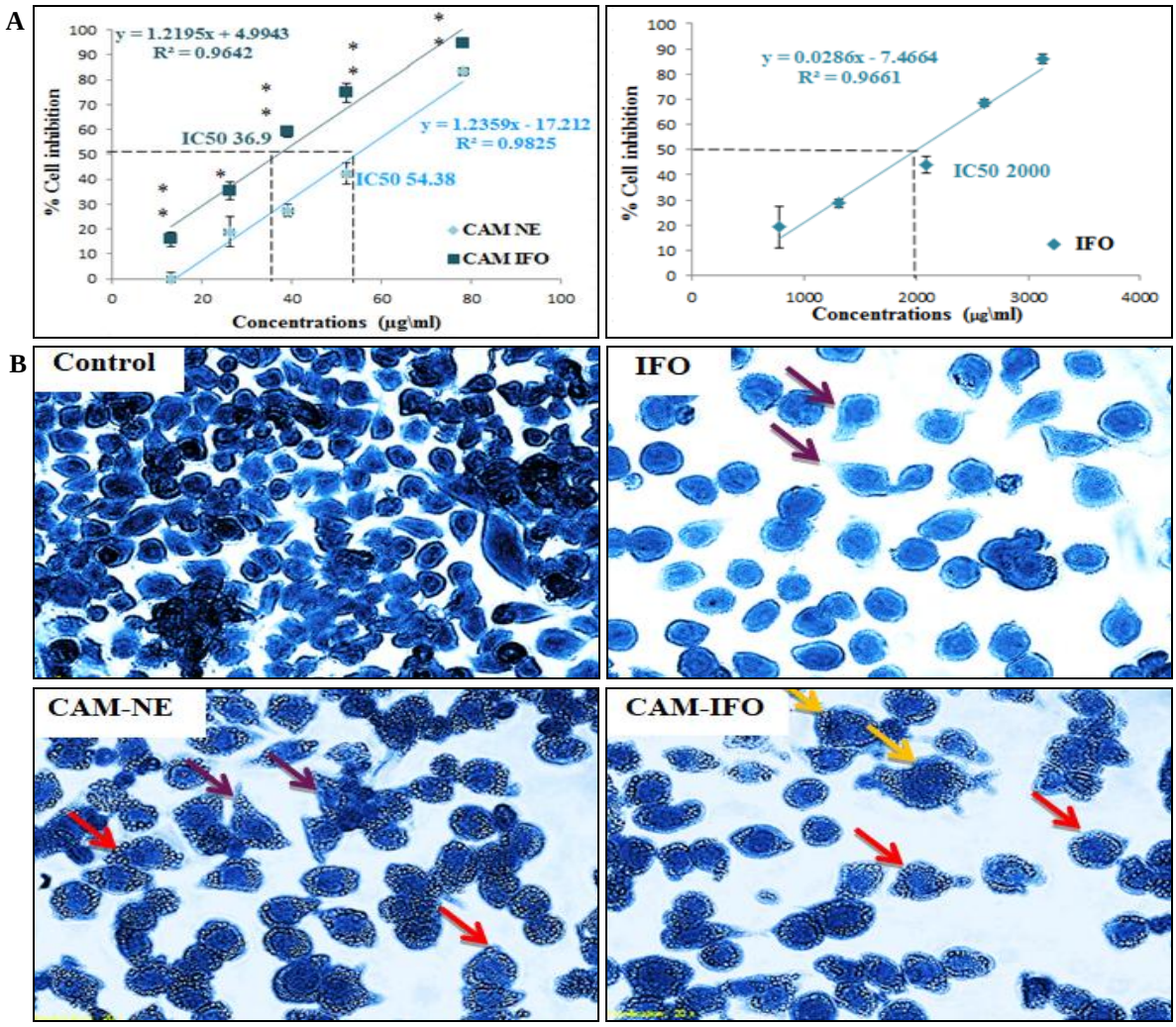

FIG 3: (A) MTT ASSAY DETERMINATION OF THE PERCENTAGES OF HeLa CELLS GROWTH INHIBITION SUBJECT INTO THE TESTED FORMULAS FOR 24 h AT DIFFERENT CONCENTRATIONS OF CAM-NE, CAM-IFO, AND IFO. (B) LIGHT MICROSCOPY IMAGES OF THE UNTREATED HeLa CELLS (CONTROL) AND THE TREATED HELA CELLS WITH THE IC_{50}'s OF 2000, 54.38 AND 36.90 µg/ml FOR IFO, CAM-NE, AND CAM-IFO, RESPECTIVELY. Error bars display the standard deviation; *P*-values were measured by the independent *t*-test; * P<0.05; ** 0.001<P<0.05. Images were magnified at 400X. Purple, red and oranges arrows represent membrane blebbing, vesicles and cell enlargement, respectively.

Nuclear Morphology Changes: To evaluate the apoptotic effects of the tested formulas on the cellular nuclei at different concentration following 24 h incubation, MCF-7 and HeLa cells were stained with DAPI. In general, it has been found that as the tested formula concentration increased the nuclear staining of the desired cells, expressed as the % of cellular uptake, decreased indicating that the chromatids have got fragmented **Fig. 4A** and **5A**. The maximum effect on the cellular uptake

was noticed when the cells were treated with CAM-IFO while the least effect was observed in the cells treated with the free IFO. As displayed in **Fig. 4B**, the nuclear size of the MCF-7 cells treated with IC_{50}'s of CAM-NE and CAM-IFO have got decreased and condensed when compared with the nuclei of the cells treated with the IC_{50} of the free IFO. In contrast, the shape of the nuclei of the HeLa cells subjected into the IC_{50}'s of CAM-IFO and CAM-NE have magnificently enlarged and fluoresced when compared to the cells subjected into the IC_{50} of the free IFO **Fig. 5B**.

DISCUSSION: Essential oils as an antitumor agent have been investigated recently since they have many beneficial properties such as anti-proliferation, anti-inflammatory, and antimicrobial activity. Essential oils have a permeable cell membrane and act on various cellular targets involved in different pathways. ESSOs increase levels of intracellular reactive oxygen species and reactive nitrogen species which results in impeding cancer cell proliferation and metastasis leading to apoptosis in cancer cells. Also, downregulation/ corresponding up of different significant biomolecules, as well as related genes, is caused by inhibition of Akt, mTOR and mitogen-activated protein kinase (MAPK) pathways at various steps.

Furthermore, ESSOs induce apoptosis pathway through interfering with several steps in apoptosis pathway in cancer cells [21, 22, 23, 24, 25, 26]. Recent studies have also elaborated the antitumor activity of NE-based essential oils in Ehrlich ascites bearing mice [27, 28, 29, 30].

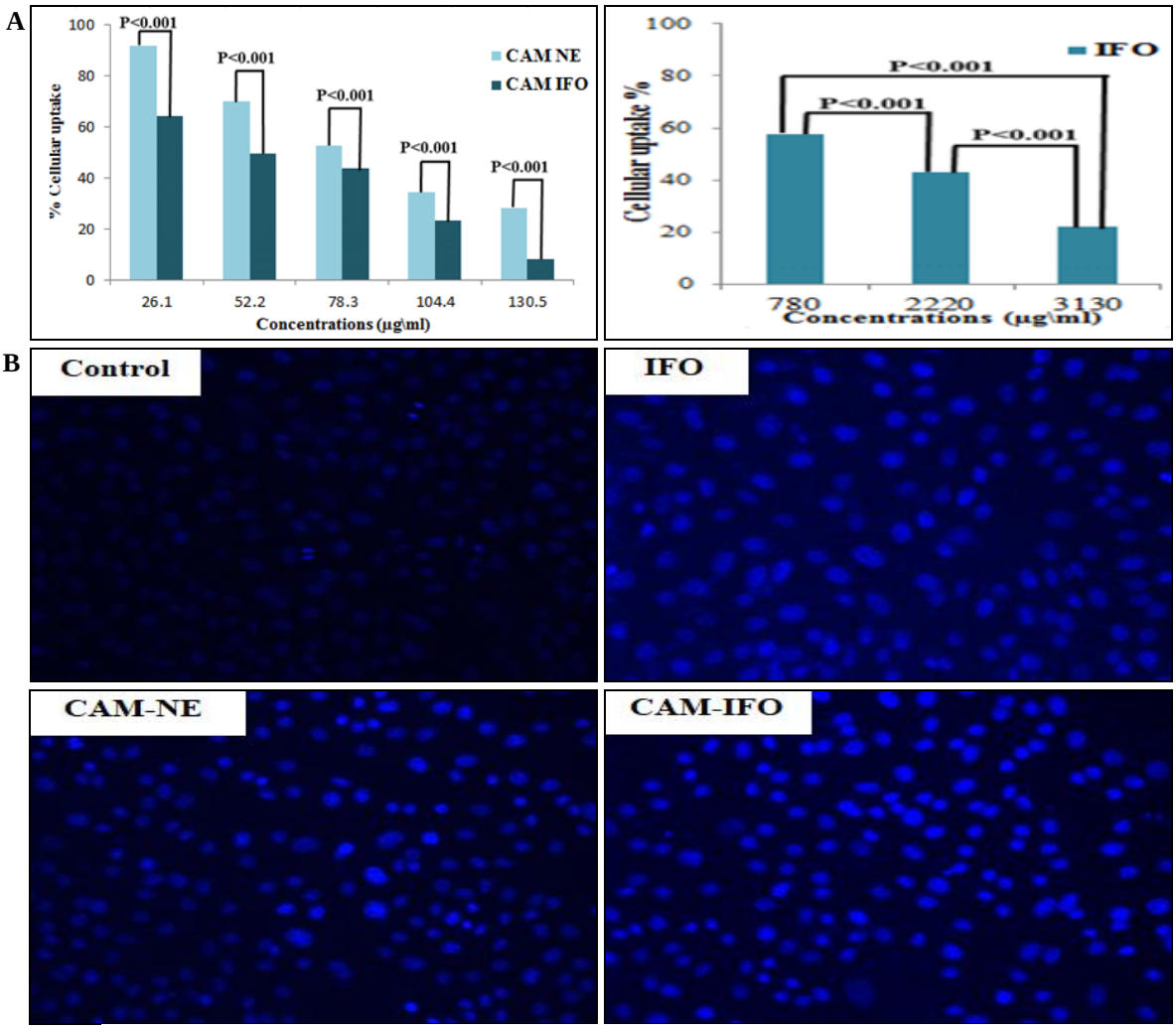

FIG. 4: DAPI NUCLEAR STAINING OF MCF-7 CELLS SUBJECTED INTO THE TESTED FORMULAS FOR 24 h. (A) Graphs showing the percentages of cellular uptake, measured from the cellular fluorescent intensities using Image J 1.43 n, at different concentrations of the tested formulas. P-values were measured by the independent t-test. (B) Fluorescent microscopy images of MCF-7 cells treated with the IC_{50}'s of the tested formulas at magnification 20 × (Scale bar = 20 µm).

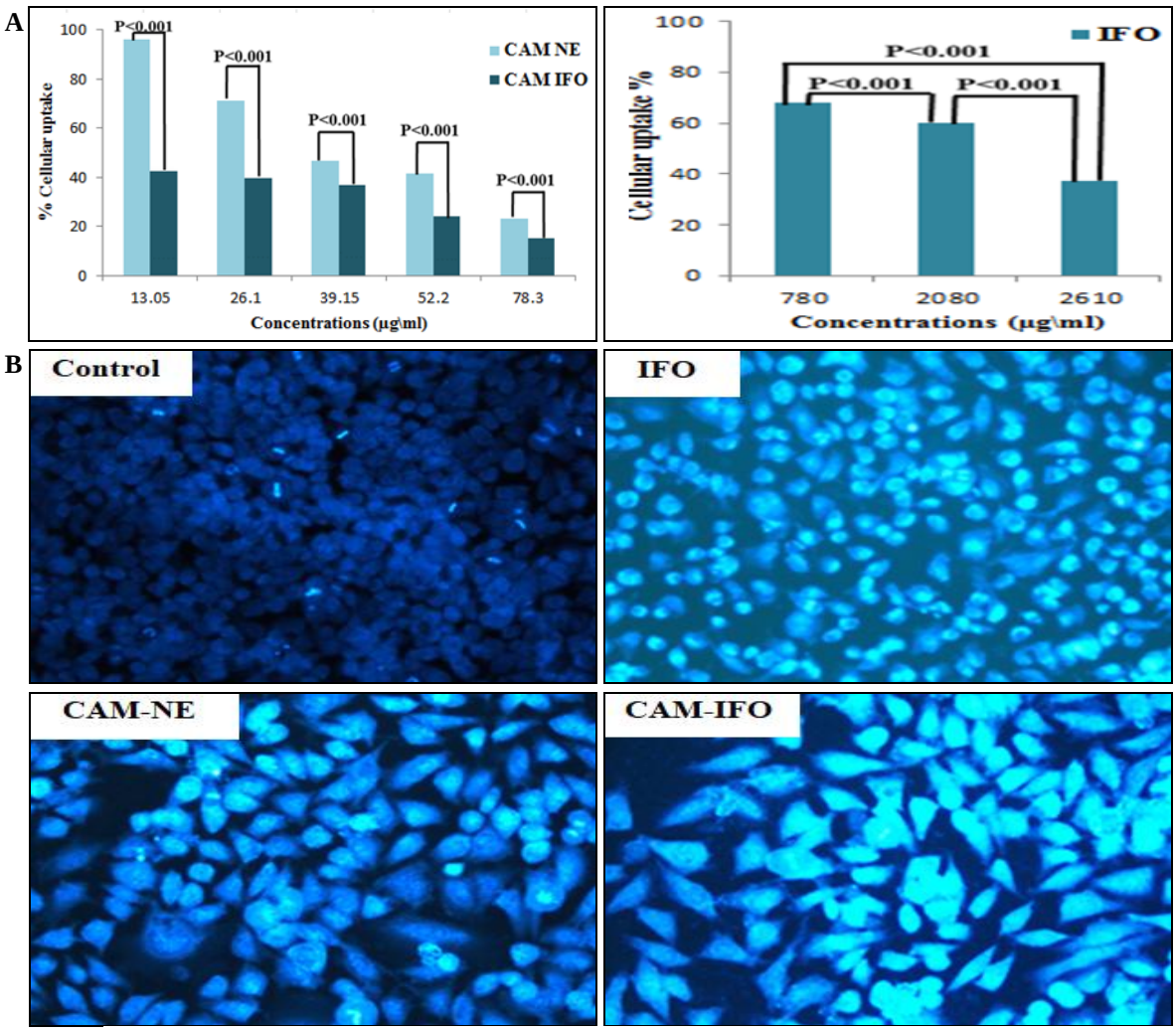

FIG. 5: DAPI NUCLEAR STAINING OF HeLa CELLS SUBJECTED INTO THE TESTED FORMULAS FOR 24 h. (A) Graphs showing the percentages of cellular uptake, measured from the cellular fluorescent intensities using ImageJ 1.43 n, at different concentrations of the tested formulas. P-values were measured by the independent *t*-test. (B) Fluorescent microscopy images of HeLa cells treated with the IC_{50}'s of the tested formulas at magnification 20 × (Scale bar = 20 µm)

The present study has introduced the formulation of IFO in NE-based CAM oil by blending different weight fractions of 1.8% CAM oil, 5.5% tween 80/ span 20 and 92.7% water. It has been demonstrated that zeta potential can determine the nanoparticles incorporated within the center or on the surface [31, 32]. In the current study, the physical characterization of CAM-IFO and CAM-NE revealed that IFO was located inside the CAM-NE since the size of CAM-NE dispersed droplets and the magnitude of their negatively charged zeta potential have considerably enlarged [33, 34, 35]. The increasing of the negative charge of the particles and the diameter of droplets after drug incorporated implies that the drug was localized inside the droplets and not on the surface.

Also, it has been demonstrated that the apoptotic effect of IFO was significantly ameliorated when loaded in CAM-NE, which was found to have greater antiproliferative activity than the free IFO. It can be attributed to the capacity of the NE structure to protect IFO as well as CAM oil from hydrolysis and enzymatic degradation [36]. Also, the size and charge of the NE nanodroplets facilitate the permeation of the IFO and CAM oil into the cells [37]. Furthermore, the anti-neoplastic activity of CAM-NE can be explained by the presence of CAM oil which was found to have anticancer activity in MCF-7 cells and colon cancer cells [38, 39].

Camphor exhibits some biological properties such as insecticidal, anti-microbial, anti-viral, anticoccidial, anti-nociceptive, anti-cancer and anti-tussive activities, in addition to its use as a skin penetration enhancer [12]. In 2014, De Lima *et al.*, [40] have reported that the inclusion of camphor in *Ocimum kilim* and *scharicum* played a major role in its anti-proliferation activity against OVCAR-3

ovarian cells. Previous studies have revealed that the anti-neoplastic effect of CAM can be due to its potential to activate the natural killer cells and sensitize radiotherapy in cancer treatment [12]. In 2016, Wu *et al*., [41] have determined the constituents that may potentiate the antitumor activity of CAM which was mainly terpinene-4-ol, α-terpineol, and safrole.

CONCLUSION: The resulted formula of CAM-IFO exhibited highly remarkable cell growth inhibition and apoptotic effects in vitro when compared to non-loaded CAM-NE and drug-free IFO. Combining IFO with CAM in NE has improved the antineoplastic efficacy of both of IFO and CAM through ameliorating their cellular permeation into the cancer cells. Further studies are needed to determine the antitumor effect of the new formula and its adverse side effects *in-vivo*.

ACKNOWLEDGEMENT: The authors wish to express a sincere thanks and appreciation to King Abdulaziz City for Science and Technology for its financial support to the research project designated by the number (1-17-01-009-0068).

AUTHOR CONTRIBUTIONS: M.H.A. and S.M.A. have written the concept of the study and designed the experiments. S.M.A. has performed the experiments. M.H.A. and S.M.A. have analyzed and interpreted the data. All authors have drafted and revised the manuscript. The whole study was performed under the supervision of M.H.A. and H.M.A.

COMPETING INTEREST: The authors declare no competing interests.

REFERENCES:

1. Kerbusch T, de Kraker J, Keizer HJ, van Putten JW, Groen HJ, Jansen RL, Schellens JH and Beijnen JH: Clinical pharmacokinetics and pharmacodynamics of Ifosfamide and its metabolites. Clinical Pharmacokinetics 2001; 40: 41-62.
2. Barakat RR, Markman M and Randall M: Principles and Practice of Gynecologic Oncology. Wolters Kluwer Health/Lippincott Williams & Wilkins Fifth Edition 2009.
3. Mioduszewska K, Dołżonek J, Wyrzykowski D, Kubik Ł, Wiczling P, Sikorska C, Toński M, Kaczyński Z, Stepnowski P and Białk-Bielińska A: Overview of experimental and computational methods for the determination of the pKa values of 5-fluorouracil, cyclophosphamide, ifosfamide, imatinib and methotrexate. TrAC Trends in Analytical Chemistry 2017; 97: 283-296.
4. Velmurugan R and Nair KG: Ifosfamide drug stability: A formulation challenge. Drug Invention Today 2018; 10: 347-351.
5. Velmurugan R and Selvamuthukumar S: Development and optimization of ifosfamide nanostructured lipid carriers for oral delivery using response surface methodology. Applied Nanoscience 2016; 6: 159-173.
6. Nakata H, Miyazaki T, Iwasaki T, Nakamura A, Kidani T, Sakayama K, Masumoto J and Miura H: Development of tumor-specific caffeine-potentiated chemotherapy using a novel drug delivery system with Span 80 nano-vesicles. Oncology Reports 2015; 33: 1593-1598.
7. Chen B, Yang JZ, Wang LF, Zhang YJ and Lin XJ: Ifosfamide-loaded poly (lactic-co-glycolic acid) PLGA-dextran polymeric nanoparticles to improve the antitumor efficacy in Osteosarcoma. BMC Cancer 2015; 15: 752.
8. Pandit AA and Dash AK: Surface-modified solid lipid nanoparticulate formulation for ifosfamide: development and characterization. Nanomedicine 2011; 6: 1397-1412.
9. Ujhelyi Z, Kalantari A, Vecsernyés M, Róka E, Fenyvesi F, Póka R, Kozma B and Bácskay I: the enhanced inhibitory effect of different antitumor agents in self-microemulsifying drug delivery systems on human cervical cancer HeLa cells. Molecules 2015; 20: 13226-13239.
10. Mou D, Chen H, Du D, Mao C, Wan J, Xu H and Yang X: Hydrogel-thickened nanoemulsion system for topical delivery of lipophilic drugs. International Journal of Pharmaceutics 2008; 353: 270-276.
11. Biswal B, Karna N, Nayak J and Joshi V: Formulation and evaluation of microemulsion based topical hydrogel containing lornoxicam. Journal of Applied Pharmaceutical Science 2014; 4: 077-084.
12. Chen W, Vermaak I and Viljoen A: Camphor-a fumigant during the black death and a coveted fragrant wood in ancient Egypt and Babylon-a review. Molecules 2013; 18: 5434-5454.
13. Weiss J, Gaysinsky S, Davidson M and McClements J. Global Issuesin Food Science and Technology. Academic Press, New York, Edition 1, Vol. I, 2009: 425-479.
14. Mahato R: Nanoemulsion as a targeted drug delivery system for cancer therapeutics. Journal of Pharmaceutical Sciences and Pharmacology 2017; 3: 83-97.
15. Gurpreet K and Singh S: Review of nanoemulsion formulation and characterization techniques. Indian Journal of Pharmaceutical Sciences 2018; 80: 781-789.
16. Primo FL, Rodrigues MM, Simioni AR, Bentley MV, Morais PC and Tedesco AC: *In-vitro* studies of cutaneous retention of magnetic nanoemulsion loaded with zinc phthalocyanine for synergic use in skin cancer treatment. Journal of Magnetism and Magnetic Materials 2008; 320: e211-e214.
17. Devalapally H, Zhou F, McDade J, Goloverda G, Owen A, Hidalgo IJ and Silchenko S: Optimization of PEGylated nanoemulsions for improved pharmacokinetics of BCS class II compounds. Drug Delivery 2015; 22: 467-474.
18. Silva AE, Barratt G, Chéron M and Egito EST: Development of oil-in-water microemulsions for the oral delivery of amphotericin B. International Journal of Pharmaceutics 2013; 454: 641-648.
19. Porras M, Solans C, González C, Martínez A, Guinart A and Gutiérrez JM: Studies of formation of W/O nano-emulsions. Colloids and Surfaces A: Physicochemical and Engineering Aspects 2004; 249: 115-118.
20. Zhao Y, Wang Z, Zhang W and Jiang X: Adsorbed tween 80 is unique in its ability to improve the stability of gold

nanoparticles in solutions of biomolecules. Nanoscale 2010; 2: 2114-2119.

21. Wang Q, Pan LH, Lin L, Zhang R, Du YC, Chen H, Huang M, Guo KW and Yang XZ: Essential Oil from *Carpesium abrotanoides* Linn. induces apoptosis *via* activating the mitochondrial pathway in hepatocellular carcinoma cells. Current Medical Science 2018; 38: 1045-1053.
22. Chang WL, Cheng FC, Wang SP, Chou ST and Shih Y: *Cinnamomum cassia* essential oil and its major constituent cinnamaldehyde induced cell cycle arrest and apoptosis in human oral squamous cell carcinoma HSC-3 cells. Environmental Toxicology 2017; 32: 456-468.
23. Ma JW, Tsao TCY, Hsi YT, Lin YC, Chen Y, Chen Y, Ho CT, Kao JY and Way TD: Essential oil of *Curcuma aromatica* induces apoptosis in human non-small-cell lung carcinoma cells. Journal of Functional Foods 2016; 22: 101-112.
24. Chen H, Zhou B, Yang J, Ma X, Deng S, Huang Y, Wen Y, Yuan J and Yang X: Essential oil derived from *Eupatorium adenophorum* Spreng. mediates anticancer effect by inhibiting STAT3 and AKT activation to induce apoptosis in hepatocellular carcinoma. Frontiers in Pharmacology 2018; 9: 483.
25. Gautam N, Mantha AK and Mittal S: Essential oils and their constituents as anticancer agents: a mechanistic view. Bio Med Research International 2014; 2014: 154106.
26. Blowman K, Magalhães M, Lemos M, Cabral C and Pires I: Anticancer properties of essential oils and other natural products. Evidence-Based Complementary and Alternative Medicine 2018; Article ID 3149362: 1-12.
27. Alkhatib MH, Nori DA and Al-Ghamdi MA: Antitumor activity and hepatotoxicity effect of sorafenib-incorporated into nanoemulsion formulated with flaxseed oil. International Journal of Pharmaceutical Research and Allied Sciences 2017; 6: 175-188.
28. Alkhatib MH, Binsiddiq BM and Backer WS: *In-vivo* evaluation of the anticancer activity of a water-in-garlic oil nanoemulsion loaded with docetaxel. International Journal of Pharmaceutical Sciences & Research 2017; 8: 5373-79.
29. Alkhatib MH, Alharbi SA and Mahassni SH: *In-vivo* evaluation of the anticancer activity of the docetaxel incorporated into nanoemulsion-based on orange oil. Pharmacophore 2017; 8: 41-47.
30. Alkhatib MH, Alnahdi NS and Backer WS: Antitumor activity, hematoxicity and hepatotoxicity of sorafenib formulated in a nanoemulsion-based on the carrot seed oil. International Journal of Life Science and Pharma Research 2018; 8: 50-57.
31. Honary S, Jahanshahi M, Golbayani P, Ebrahimi P and Ghajar K: Doxorubicin-loaded albumin nanoparticles: formulation and characterization. Journal of Nanoscience and Nanotechnology 2010; 10: 7752-7757.
32. Honary S, Ebrahimi P, Tabbakhian M and Zahir F: Formulation and characterization of doxorubicin nano-vesicles. Journal of Vacuum Science & Technology B: Microelectronics and Nanometer Structures Processing, Measurement, and Phenomena 2009; 27: 1573-1577.
33. Peira E, Chirio D, Battaglia L, Barge A, Chegaev K, Gigliotti CL, Ferrara B, Dianzani C and Gallarate M: Solid lipid nanoparticles carrying lipophilic derivatives of doxorubicin: Preparation, characterization, and *in-vitro* cytotoxicity studies. Journal of Microencapsulation 2016; 33: 381-390.
34. Abdolahpour S, Mahdieh N, Jamali Z, Akbarzadeh A, Toliyat T and Paknejad M: Development of doxorubicin-loaded nanostructured lipid carriers: preparation, characterization, and *in-vitro* evaluation on MCF-7 cell line. Bio Nano Science 2017; 7: 32-39.
35. Abu-Fayyad A, Kamal MM, Carroll JL, Dragoi A-M, Cody R, Cardelli J and Nazzal S: Development and *in-vitro* characterization of nanoemulsions loaded with paclitaxel/γ-tocotrienol lipid conjugates. International Journal of Pharmaceutics 2018; 536: 146-157.
36. Thiagarajan P: Nanoemulsions for drug delivery through different routes. Research in Biotechnology 2011; 2: 1-13.
37. Honary S and Zahir F: Effect of zeta potential on the properties of nano-drug delivery systems-a review (Part 1). Tropical Journal of Pharmaceutical Research 2013; 12: 255-264.
38. Itani WS, El-Banna SH, Hassan SB, Larsson RL, Bazarbachi A and Gali-Muhtasib HU: Anti colon cancer components from lebanese sage (*Salvia libanotica*) essential oil: mechanistic basis. Cancer Biology & Therapy 2008; 7: 1765-1773.
39. Salvia-Trujillo L, Rojas-Graü A, Soliva-Fortuny R and Martín-Belloso O: Physicochemical characterization and antimicrobial activity of food-grade emulsions and nano-emulsions incorporating essential oils. Food Hydrocolloids 2015; 43: 547-556.
40. De Lima V, Vieira M, Kassuya C, Cardoso C, Alves J, Foglio M, De Carvalho J and Formagio A: Chemical composition and free radical-scavenging, anticancer and anti-inflammatory activities of the essential oil from *Ocimum kilimandscharicum*. Phytomedicine 2014; 21: 1298-1302.
41. Wu ZL, Du YH, Guo ZF, Lei KJ, Jia YM, Xie M, Kang X, Wei Q, He L and Wang Y: Essential oil and its major compounds from oil camphor inhibit human lung and breast cancer cell growth by cell-cycle arresting. International Journal of Clinical and Experimental Medicine 2016; 9: 12852-12861.

How to cite this article:
AlMotwaa SM, Alkhatib MH, Alkreathy HM: Nanoemulsion-based camphor oil carrying Ifosfamide: preparation, characterization, and *in-vitro* evaluation in cancer cells. Int J Pharm Sci & Res 2019; 10(4): 2018-26. doi: 10.13040/IJPSR.0975-8232.10(4).2018-26.